A&A 478, 921–927 (2008)
DOI: 10.1051/0004-6361:20078481

Astronomy & Astrophysics

Torsional Alfvén waves in small scale density threads of the solar corona

P. Copil, Y. Voitenko, and M. Goossens

Centre for Plasma Astrophysics, K. U. Leuven, Celestijnenelaan 200 B, 3001 Heverlee, Belgium
e-mail: copil@wis.kuleuven.be

Received 14 August 2007 / Accepted 3 December 2007

ABSTRACT

The density structuring of the solar corona is observed at large scales (loops and funnels), but also at small scales (sub-structures of loops and funnels). Coronal loops consist of thin density threads with sizes down to (and most probably below) the resolution limit. We study properties of torsional Alfvén waves propagating in inhomogeneous cylindrical density threads using the two-fluid magnetohydrodynamic equations. The eigenmode solutions supported by such a structure are obtained and analysed. It is shown that the dispersive and dissipative effects become important for the waves localised in thin threads. In this case, the Alfvén wave continuum is replaced with a discrete spectrum of Alfvén waves. This mathematical model is applied to the waves propagating in coronal structures. In particular, we consider ~1 Hz Alfvén waves propagating along density threads with a relatively smooth radial profile, where a density contrast of about 1.1 is attained at radial distances of about 0.1 km. We found that the dissipation distance of these waves is less than the typical length of hot coronal loops, 50 Mm. Torsional Alfvén waves are localised in thin density threads and produce localised heating. Therefore, these waves can be responsible for coronal heating and for maintenance of small-scale coronal structuring.

Key words. magnetohydrodynamics (MHD) – waves – methods: analytical – plasmas – Sun: corona

1. Introduction

The solar atmosphere is highly structured in density and magnetic field. The magnetic field of the Sun interacts with the plasma and determines the processes taking place in the outer solar atmosphere. The field in the atmosphere is structured in the form of open coronal funnels and closed coronal loops.

One of the early models for the magnetic field was developed by Kopp & Kuperus (1968) and Kopp (1972). These authors assumed that the field is structured only as coronal funnels. According to this model, the magnetic field lines emerge from the lanes of the chromospheric network and spread as they go upwards in the corona. This model could explain the emission of EUV lines, which shows a pattern that reproduces the granulation. Gabriel (1974) improved Kopp's model of the magnetic field by dividing the transition region into two: the primary and the secondary region. The primary transition region is located inside the funnels in the places where most of the EUV radiation comes from, while the secondary transition region is in the area between two funnels and emits only a small amount of radiation.

The initial picture was completed by introducing closed structures: coronal loops. The loops are smaller than the funnels and do not extend very high in the corona. The existence of loops can explain the difference between the magnetic field maps in the photosphere and the spectrograms in coronal lines. According to the early models, EUV images and magnetograms should have a similar pattern, strong emission being associated with strong magnetic field. However, there are regions with strong field that do not show high emission in the corona and these are the places where the loops are. This coronal magnetic field model, consisting of both closed and open structures, is commonly accepted.

In addition to the magnetic field, density is also highly structured in the corona. This can be seen in X-ray images of the corona taken from space by rockets and telescopes. Pictures from Skylab (Vaiana et al. 1973) revealed that the coronal plasma is concentrated mostly in the loops. More recent pictures, taken by TRACE, show that coronal loops are not uniform, but consist of thin threads with sizes down to the resolution limit. Based on these observations, Reale & Perez (2000) constructed a model in which loops are considered to be made of bundles of threads, independent of each other and in different physical conditions. Aschwanden & Nightingale (2005) made a quantitative study on the multithread coronal loops and concluded that the elementary isothermal thread of the loop has a width of about 2000 km. It is possible that the isothermal thread has a finer density structuring, which cannot be observed because the size of the structures is smaller than the resolution limit. In this paper, we consider that the isothermal thread consists of multiple thinner density striations, which we regard as the elementary threads of the loop.

In solar physics and heliospheric physics, studies of magnetohydrodynamic (MHD) waves in the 1970 s and 1980 s were motivated by: (1) the observation of Alfvén waves in the solar wind (Belcher & Davis, 1971; see also review by Hollweg 1990), (2) the anticipation due to theoretical arguments that the various magnetic structures in the solar atmosphere had to support MHD waves (e.g. Spruit 1982; Roberts et al. 1984), and (3) the possibility that MHD waves contribute to the heating of the solar corona (Hollweg & Yang 1988; Grossmann & Smith 1988; Poedts et al. 1989, 1990).

The theory of waves in magnetic structures was initiated by Roberts et al. (1984) more than 20 years ago. They modelled

the coronal loop as a straight cylinder with constant plasma density and constant magnetic field in the interior, as well as in the exterior. Applying the MHD wave theory to this loop model, the authors discovered that such a structure can support a diversity of modes, which are classified in two groups: Alfvén waves and magnetosonic waves. The Alfvén waves propagate along the equilibrium magnetic field and their perturbations are perpendicular to the propagation vector. In cylindrical geometry with axial magnetic field, there exist Alfvén waves with only azimuthal components for the magnetic field and velocity perturbations. These waves are called the torsional Alfvén waves. They are axis symmetric modes, with the azimuthal wavenumber $m = 0$, so they do not produce pressure or density variations. For the gas/magnetic pressure ratio $\beta < 1$, the magnetosonic waves have two classes of modes of oscillation: slow mode (propagating with a velocity close to the sound speed) and fast mode (propagating with a velocity close to the Alfvén speed). The slow and fast modes are also classified relative to the azimuthal wave number, m, as sausage ($m = 0$), kink ($m = 1$) and flute modes ($m \geq 2$). The sausage mode is symmetric about the axis of the cylinder, while the kink mode in antisymmetric. After the launching of solar telescopes SOHO and TRACE, an enormous amount of data became available, which can be compared with the theory.

Torsional modes are difficult to observe because, as they are incompressible, the density is not perturbed, so they cannot be seen in variations of the emission lines. However, torsional Alfvén waves can be detected by measuring the broadening of emission lines due to the Doppler effect. Early observations with Skylab show that the line widths increase with height above the limb. More recent observations, performed with SOHO (Banerjee et al. 1998; Doyle et al. 1999) in coronal holes, also show a line broadening up to 1.2 solar radii, then a constant profile up to 1.5 solar radii and then a sharp increase. In the equatorial quiet Sun (Harrison et al. 2002) a narrowing of coronal lines above 50 000 km was noticed. This was considered as the first evidence of dissipation of shear Alfvén waves. However, contrary to Harrison, the results obtained by Wilhelm et al. (2004) indicate a broadening of the line with height in both the equatorial part and polar coronal holes. Zaqarashvili (2003) suggested a method to calculate the velocity of standing torsional Alfvén waves, by measuring the wavelength and the period from spectral observations. The wavelength is two times the distance between two antinodes, which exhibit a line broadening in the spectrum, while the period is measured taking spectra at different times at the same height.

Torsional Alfvén waves can be used as a tool for coronal seismology. In a recent paper, Zaqarashvili & Murawski (2007) obtained the dispersion relation and the wave profile for standing torsional Alfvén wave in a coronal loop with varying density along the loop. Knowing the wave frequency from spectral measurements, the loop length and the inhomogeneity parameter, the Alfvén velocity at the loop apex can be calculated, and afterwards the magnetic field.

In this paper we study the propagation and dissipation of torsional Alfvén waves in the elementary density structures of the corona. The waves are assumed to be launched at the coronal base.

The paper is structured as follows. In Sect. 2 we present the model for the density thread and we write the equations used to describe the wave supported by the thread. We then derive the governing equation for the wave propagation. In Sect. 3 we look for a solution to the wave equation. Choosing an appropriate profile for the Alfvén velocity, an analytical solution for the equation is found, after making some approximations. The dispersion relation is obtained numerically. In Sect. 4 we investigate the wave damping due to viscosity and resistivity and we compute the value for the damping distance in coronal conditions. Section 5 contains the discussion and conclusions.

2. Plasma model and basic equations

We model the elementary density structure in the corona by a cylindrical tube with enhanced density. In the interior of the tube, up to a radius R, the plasma is homogeneous and it is characterised by constant plasma parameters: density, pressure and magnetic field. The magnetic field is straight and in the z direction. For $r > R$ the plasma density decreases, but the magnetic field remains constant.

In order to keep the pressure balance in the inhomogeneous region, the magnetic pressure must also vary, together with the gas pressure. This happens only if the magnetic field is inhomogeneous, which is contrary to the assumption made above. However, since in the corona the plasma β is very low, only a small change in the magnetic field produces a considerable increase of magnetic pressure, which balances the decrease of gas pressure. The change in the magnetic field is so small that we can consider the field to be constant everywhere.

Our purpose is to study the propagation of torsional Alfvén waves with $m = 0$ in elementary density structures. We use the two-fluid model for the plasma to calculate the profile of the wave and the dispersion relation. We then compare the results with the torsional Alfvén wave in the previously studied MHD model. In ideal MHDs, the picture of the Alfvén wave is very simple: an hydrodynamic-electromagnetic wave, which propagates along the magnetic field lines. The plasma oscillates perpendicular to the magnetic field and there are also oscillations of electric and magnetic field coupled with the plasma motion. The restoring force is the magnetic tension, which is balanced by the inertia of ions and there are no pressure changes associated with the wave. It propagates at the Alfvén velocity, $v_{\rm A} = B_0/\sqrt{4\pi\rho_0}$, which depends on the local values of the equilibrium density, ρ_0 and magnetic field, B_0.

Looking at the Alfvén wave in the framework of the two-fluid model, its picture becomes more complicated than in ideal MHDs. In this case, there are pressure modifications in the equations, which lead to new and interesting effects. Accounting for electron parallel dynamics (electron pressure) and cross-field ion dynamics (ion gyroradius), the picture of the Alfvén wave complicates with the inclusion of a parallel electric field and parallel motions of the electrons.

The two-fluid MHD equations are:

$$n_{\rm i} m_{\rm i} \frac{{\rm d}\boldsymbol{v}_{\rm i}}{{\rm d}t} = q_{\rm i}\boldsymbol{E} + \frac{q_{\rm i}}{c}\boldsymbol{v}_{\rm i} \times \boldsymbol{B} - \nabla p_{\rm i}; \tag{1}$$

$$n_{\rm e} m_{\rm e} \frac{{\rm d}\boldsymbol{v}_{\rm e}}{{\rm d}t} = q_{\rm e}\boldsymbol{E} + \frac{q_{\rm e}}{c}\boldsymbol{v}_{\rm e} \times \boldsymbol{B} - \nabla p_{\rm e}; \tag{2}$$

$$\frac{\partial n_{\rm i}}{\partial t} + \nabla\cdot(n_{\rm i}\boldsymbol{v}_{\rm i}) = 0; \tag{3}$$

$$\frac{\partial n_{\rm e}}{\partial t} + \nabla\cdot(n_{\rm e}\boldsymbol{v}_{\rm e}) = 0; \tag{4}$$

$$\nabla\cdot\boldsymbol{B} = 0; \tag{5}$$

$$\nabla\cdot\boldsymbol{E} = 4\pi e(n_{\rm i} - n_{\rm e}); \tag{6}$$

$$\nabla\times\boldsymbol{B} = \frac{4\pi}{c}\boldsymbol{j}; \tag{7}$$

$$\nabla\times\boldsymbol{E} = -\frac{1}{c}\frac{\partial\boldsymbol{B}}{\partial t}, \tag{8}$$

where the indices i and e refer to ions and electrons, $\boldsymbol{v}$ is the velocity, p is the gas pressure, n the number density, $\boldsymbol{E}$ the electric field, $\boldsymbol{B}$ the magnetic field, $\boldsymbol{j}$ the current, q_i the ion charge density, q_e the electron charge density, c the speed of light in vacuum and e the elementary charge.

In what follows, it is more convenient to write the magnetic and electric fields with the use of the scalar potential, ϕ and vector potential, $\boldsymbol{A}$, as:

$$\boldsymbol{E} = -\nabla\phi - \frac{1}{c}\frac{\partial\boldsymbol{A}}{\partial t}; \tag{9}$$

$$\boldsymbol{B} = \nabla\times\boldsymbol{A}. \tag{10}$$

We look for a solution in the form of linear waves and we write each of the quantities as a sum of an equilibrium quantity and a perturbed quantity:

$$\boldsymbol{A} \rightarrow \boldsymbol{A_0} + \boldsymbol{A}; \tag{11}$$

$$\phi \rightarrow \phi_0 + \phi. \tag{12}$$

Since we focus on torsional waves, we assume that the perturbation of the magnetic field is different from zero only in the φ direction.

After some algebra (see Appendix), Eqs. (1)–(8) become decoupled and reduce to the following equation for the z component of the magnetic potential:

$$\frac{\partial}{\partial r}\left[r\rho_\mathrm{i}^2\frac{\partial}{\partial r}\frac{\partial^2}{\partial z^2}\triangle_\perp A_z + n_0 r\rho_\mathrm{s}^2\frac{\partial}{\partial r}\frac{\partial^2}{\partial z^2}\frac{1}{n_0}\triangle_\perp A_z + r\left(\frac{1}{v_\mathrm{A}^2}\frac{\partial^2}{\partial t^2} - \frac{\partial^2}{\partial z^2}\right)\frac{\partial A_z}{\partial r}\right] = 0, \tag{13}$$

where ρ_i is the ion gyroradius, ρ_s is the ion gyroradius at the electron temperature, v_A is the Alfvén velocity and n_0 is the equilibrium number density.

In the derivation of this equation we assumed that $\lambda_\mathrm{i}^2\partial_z^2 \ll 1$, where $\lambda_\mathrm{i} = c\sqrt{m_i/4\pi n_0 e^2}$ is the ion skin depth. With this condition we neglect the cyclotron effects and study only the waves with frequencies much smaller than the ion cyclotron frequency. Since the ion cyclotron frequency is of the order of 10^5 Hz, this approximation is valid for all waves with frequencies below 10^4 Hz.

Equation (13) governs the behaviour of the torsional Alfvén waves with $m = 0$. After solving it and finding A_z, we can calculate other quantities related to the wave.

In the framework of ideal MHD theory, the solution for torsional Alfvén waves is well known (Ruderman et al. 1997a). The waves propagate locally, on surfaces of constant flux, and the phase speed varies with space, $\omega/k = v_\mathrm{A}(r_0)$. According to this relation, the frequency spectrum of the waves is continuous. The eigenfunctions are any functions for the interior homogeneous region and delta functions, $\delta(r - r_0)$, for the inhomogeneous region. The delta functions are singular at the magnetic surface with $r = r_0$ and zero everywhere else in space, therefore they are localised. In the next section we will see that the thermal effects, taken into account with the two-fluid approach, remove the singular continuous spectrum and introduce a non-singular discrete spectrum for torsional Alfvén waves. Torsional Alfvén waves were studied in dissipative MHD for 1D cylindrical magnetic tubes by Ruderman et al. (1997a). Ruderman et al. (1997b) studied them in a 2D coronal arcade model as a possible heating mechanism. In 3D, the first nonlinear resistive MHD simulations of coronal loop heating by resonant absorption of Alfvén waves were done by Ofman & Davila (1995). In the present paper we go beyond the classic ideal and dissipative MHD formulation of torsional Alfvén waves. In view of very short length scales of density structures across the coronal loops we adopt a two-fluid formulation of torsional Alfvén waves. The most important finding is that the continuum of frequencies with Alfvén waves living on each magnetic surface is replaced by a finite number of discrete torsional Alfvén waves.

3. Solutions of wave equation

In this section we look for a solution to Eq. (13), in order to determine the wave profile and to calculate the dispersion relation.

After Fourier-analysing in z, we consider the solution in the form of one-Fourier harmonic:

$$\frac{\partial}{\partial r}A_z(r,z,t) = \frac{\partial}{\partial r}A(r)\mathrm{e}^{\mathrm{i}(kz-\omega t)}, \tag{14}$$

where ω is the frequency of the wave, k is the wavenumber in the z direction, and $A = A(r)$ is the wave amplitude dependent on r.

Introducing the solution into Eq. (13), we obtain the following differential equation for A:

$$\frac{\partial}{\partial r}\left[r\rho_\mathrm{i}^2\frac{\partial}{\partial r}\triangle_\perp A + n_0 r\rho_\mathrm{s}^2\frac{\partial}{\partial r}\frac{1}{n_0}\triangle_\perp A + r\left(\frac{\omega^2}{k^2 v_A^2} - 1\right)\frac{\partial A}{\partial r}\right] = 0. \tag{15}$$

We make all the quantities dimensionless, i.e. the distances by $\sqrt{\rho_\mathrm{i}^2 + \rho_\mathrm{s}^2}$, the magnetic field by the equilibrium magnetic field, the velocities by the Alfvén velocity in the interior region, the density by 4π multiplied by the density in the interior region. We take into account that for a smooth density variation $n_0/r \ll 0.5\cdot\mathrm{d}n_0/\mathrm{d}r$ and use the notation $\psi(r) = \mathrm{d}A(r)/\mathrm{d}r$ to write Eq. (15) as:

$$\frac{\partial^2}{\partial r^2}\Psi + \frac{1}{r}\frac{\partial}{\partial r}\Psi + \left(\frac{\omega^2}{k^2 v_\mathrm{A}^2(r)} - 1 - \frac{1}{r^2}\right)\Psi = \frac{c}{r}\cdot \tag{16}$$

Equation (16) is an eigenmode equation, in which Ψ is the eigenfunction and ω/k is the eigenvalue.

First, we choose a particular profile for the Alfvén velocity, v_A, then we look for a solution to Eq. (16). In order to keep the equation simple and tractable analytically, we adopt the following r-dependence:

$$v_\mathrm{A}(r) = \begin{cases} 1, & r \le R; \\ \frac{R+1}{R}\frac{r}{r+1}, & R < r. \end{cases} \tag{17}$$

The profile for the Alfvén velocity is shown in Fig. 1. According to this model, the density is constant inside the tube up to a radius R, then the density decreases slowly. The size of the structure is the length over which the density varies significantly, and in our case it is about 0.1 km. This should not be confused with the radius of the homogeneous region, R, which is about 10 m.

With this profile for the Alfvén velocity, the solutions of Eq. (16) are:

$$\Psi(r) = \begin{cases} a_1 J_1(\mu_1 r), & r \le R; \\ b_1 W_{\frac{1-\mu_2^2}{\mu_2},\mu_2}(2\mu_2 r), & R < r, \end{cases} \tag{18}$$

where J_1 is an ordinary Bessel function of the first kind, W is a Whittaker function, $\mu_1 = \sqrt{(\omega/k)^2 - 1}$ is the radial wavenumber for $r \leq R$, $\mu_2 = \sqrt{1 - (\omega/k)^2 R^2/(R+1)^2}$ is the radial wavenumber for $R < r$, and a_1 and b_1 are real arbitrary constants.

To obtain a solution for the whole interval, we have to connect the solutions obtained in the two regions and impose the boundary conditions at $r = 0$ and at $r \to \infty$. These conditions are:

- the solution must be regular at the origin;
- the solution has to be zero at infinity (with this condition we consider only confined waves and exclude leaky waves);
- the solution and its first derivatives have to be continuous at $r = R$.

By connecting the solutions and its first derivatives, we impose the continuity of physical quantities, such as: the magnetic field (proportional to the solution itself), the current in the z direction, j_z and the electric field in the z direction, E_z (both proportional to the solution and its first derivative).

From these conditions we can calculate b_1 in terms of a_1 and obtain the dispersion relation. In our case, it is a transcendental equation in ω/k, which can be solved numerically. The numerical solutions obtained for ω/k indicate that the wave spectrum is discrete in phase velocity. The nature of the discrete spectrum is due to the boundary conditions. In this way, the geometry of the physical system "chooses" the characteristics of the wave that propagates in it, or the wave propagates only if it is allowed by the shape of the medium.

We present some results obtained for the following parameters: $B_0 = 50$ G, $T_\mathrm{i} = T_\mathrm{e} = 2 \times 10^6$ K, $n_0 = 3 \times 10^9$ cm^{-3}. We choose the inner radius of the cylinder to be $R = 10$ (in effective gyroradii).

From Fig. 1 we see that the Alfvén velocity has the value 1 in the interior of the cylinder, up to a radius $R = 10$; for $r > R$ it increases slowly as $1.1r/(r+1)$, going asymptotically to 1.1 for large r. The dots represent the values of r_0 (Alfvén resonance point in ideal MHDs) for which the dispersion relation is satisfied. The Alfvén resonance point, r_0, is related to the phase velocity, ω/k, by the formula $\omega/k = v_\mathrm{A}(r_0)$. Each dot corresponds to a wave that has a particular profile in r and propagates with its own speed. In one-fluid MHDs the wave spectrum in continuous, so there are waves propagating with any speed between 1 and 1.1, but in two-fluid MHDs only some phase speeds are allowed. The phase velocity for the first mode (called also the ground mode) is 1.03, for the second mode it is 1.06.

The possible excitation mechanisms for the ground mode, which has the largest radial wavelengths, include convective plasma motions at magnetic footpoints and magnetic restructuring at all levels from photosphere to corona. The wave profile for this mode, given by the expressions in Eqs. (18), is shown in Fig. 2. The magnetic field is zero in the centre of the cylinder, then has a maximum and decreases again to zero. The current is maximum in the centre, decreases to negative values and then goes to zero. The profiles for both the current and the magnetic field are confined in a region with the radius about 30. Therefore, the ground mode is localised in the centre of the thread, where the density is enhanced.

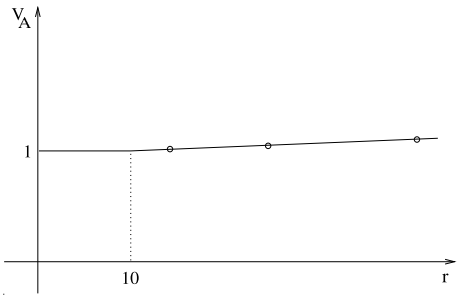

Fig. 1. Model of thread in cylindrical geometry. The plot shows the profile for the Alfvén velocity: constant until $R = 10$, then slowly increasing as $1.1r/(r+1)$. The Alfvén velocity is made dimensionless by the Alfvén velocity in the interior and the radius is expressed in gyroradii, $\sqrt{\rho_\mathrm{i}^2 + \rho_\mathrm{s}^2}$. The dots show the Alfvén resonance points in ideal MHDs.

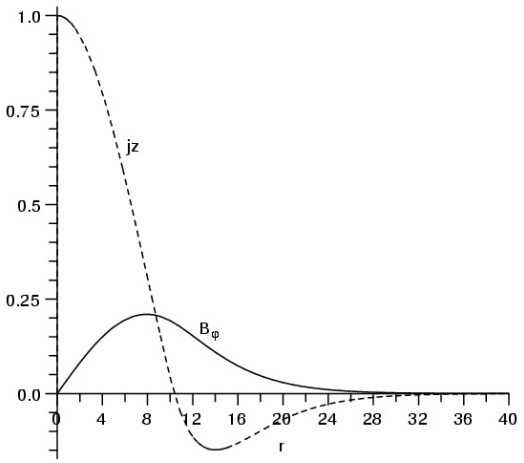

Fig. 2. Wave profile for the first mode. The plot shows the current in the z direction, j_z (dashed line), and the magnetic field in the φ direction, B_φ (full line), as a function of the distance from the centre of the cylinder. The current is normalised by the current at $r = 0$ and the magnetic field by $(\sqrt{\rho_\mathrm{i}^2 + \rho_\mathrm{s}^2}/v_\mathrm{A})j_z$ at $r = 0$.

4. Collisional dissipation of torsional Alfvén waves

To give a realistic description of the waves, we need to take into account dissipation. Voitenko & Goossens (2000) have shown that the collisionless Landau damping of ~1 Hz kinetic Alfvén waves in active regions is much weaker than the collisional damping. In this case, the main mechanisms that cause damping of torsional Alfvén waves in coronal conditions are shear viscosity and resistivity. We take into account that the ion viscosity is much higher then electron viscosity, so electron viscosity is neglected. The viscous damping occurs due to friction between ions as they move in the φ direction and collide with other ions, while the resistive damping is due to the decrease of the parallel current as the electrons collide with ions.

The damping length of the wave can be obtained by using a method adopted by Gordon & Hollweg (1983). Following Gordon & Hollweg, we equate the divergence of the Poynting flux with the volumetric heating rate and obtain the following formula for the damping distance:

$$L_z = \frac{\frac{c}{2\pi}\int E_r B_\varphi r\mathrm{d}r}{\int \frac{1}{2}\mathrm{Re}(j_z E_z^*) r\mathrm{d}r + \int \rho_0 \nu_1^\mathrm{i} \left(\frac{\partial v_\varphi}{\partial r}\right)^2 r\mathrm{d}r}, \quad (19)$$

where $\nu_1^{\rm i}$ is a coefficient of shear viscosity. The Joule heating term is given by the expression:

$$\frac{1}{2}\mathrm{Re}(j_z E_z^*) = \frac{1}{2}\frac{m_{\rm e}\widetilde{\nu}}{n_0 {\rm e}^2}|j_z|^2, \quad (20)$$

where $\widetilde{\nu}$ is proportional to electron collision frequency, $\nu_{\rm e}$, as $\widetilde{\nu} = 0.51\nu_{\rm e}$. The wave quantities in Eqs. (19) and (20) are the ones calculated neglecting dissipation. In comparison with Eq. (50) by Gordon & Hollweg, in our Eq. (19) for the dissipation distance, we dropped the thermal conduction and radiative dissipation terms, which are weak for kinetic Alfvén waves. Instead, we take into account the Joule heating, which is strong for kinetic Alfvén waves.

Equation (19) is derived using the law of conservation of electromagnetic energy. Let us consider a small volume element of the cylinder in which the Alfvén wave propagates. Quantitatively, the law of energy conservation states that the rate of energy variation in the volume element is equal to the variation of electromagnetic flux and the energy loss from the field to the particles. Since we consider damping in space, not in time, the total field energy in the volume is constant. Therefore, we can equate the negative variation of the Poynting flux to the terms that represent the energy transfer rate (through viscosity and resistivity). The field does work on the particles and accelerates them; part of the energy is given back to the field, but part of it is lost due to friction of layers of particles with different velocities (viscosity) and collisions of electrons with ions (resistivity). Because the wave profile is changing with r, there is a different amount of energy transferred at different points, such that the transfer due to the Joule effect is maximum in the centre of the cylinder, but the energy exchange due to viscosity is maximum where the velocity gradient is the biggest. Therefore, this will create small thermal anisotropies inside the plasma. The temperature gradient can be flattened, causing heating of the plasma, or it can propagate away from that region, causing cooling of the medium.

In Eq. (19), the wave quantities are averaged over time and integrated over r and z. Using this formula, we calculate numerically the damping length for a wave propagating in plasma with typical coronal parameters. They are the same as the ones used in Sect. 3: $B_0 = 50$ G, $T_{\rm i} = T_{\rm e} = 2 \times 10^6$ K, $n_0 = 3 \times 10^9$ cm^{-3}. The inner radius of the density tube is $R = 10$, made dimensionless by the effective gyroradius. Considering that the torsional Alfvén wave has a typical wavelength $\lambda = 2 \times 10^6$ m, we obtain for the damping length the value 42.5×10^6 m. Therefore, the wave decays in approximately 20 wavelengths.

Further, we investigate the dependence of the damping length on the inner radius R of the tube. In Fig. 3 we plot the damping length as a function of R and it can be seen that the damping length increases with R. This is due to the fact that the perpendicular wavelength is proportional to R, so the greater the inner radius, the bigger the wavelength and the smaller the damping.

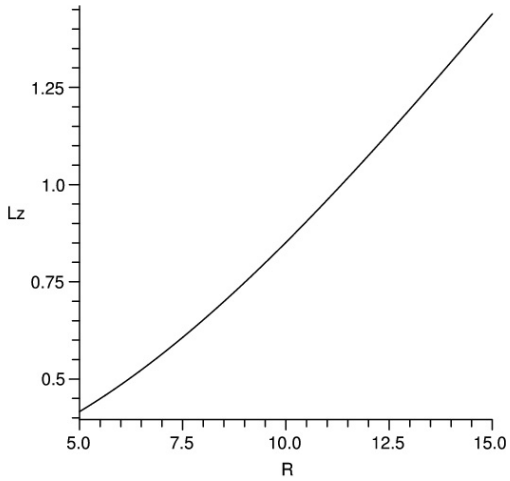

Fig. 3. Damping distance as a function of the inner radius of the density tube. The damping distance is normalised by the average length of a coronal loop, $L = 5 \times 10^7$ m, and R is expressed in gyroradii.

5. Discussion and conclusions

We found that the localised torsional Alfvén waves can exist in small-scale density threads of the solar corona. For threads modelled as density tubes, in which the density decreases from 1 at $r = 0$ to 0.97 at $r = 15$ gyroradii, the effects due to finite Larmor gyroradius are significant. The wave profile and properties of torsional Alfvén waves are very different to those found with the one-fluid MHD description. The two-fluid torsional Alfvén waves propagate along the background magnetic field and have a localised structure in the radial direction. The waves are localised in the region of density enhancement and vanish beyond the resonant point, where the local Alfvén velocity is equal to their phase velocity. Therefore, they are trapped waves, for which the elementary thread acts as a waveguide.

The solutions of the dispersion relation are discrete in phase velocity and each value of the phase velocity corresponds to a different mode, with its particular profile in the r direction. This means that the waves are dispersive with respect to the effective perpendicular wavenumber, but they are non-dispersive relative to the parallel wavenumber. These waves are kinetic Alfvén eigenmodes supported by cylindrical density tubes. For a density thread with $R = 10$ and an Alfvén velocity varying from 1 at $R = 10$ to 1.05 at $r = 20$ and going asymptotically to 1.1, there is an infinite number of modes. The wave spectrum is discrete for phase velocities below 1.1 and continuous above 1.1. The first eigenmode has the phase velocity $(\omega/k)_1 = 1.03$ and the resonance point at $r_1 = 14$, the second eigenmode has $(\omega/k)_2 = 1.06$ and $r_2 = 25$ (the Alfvén velocities and phase speeds are given relative to the interior Alfvén velocity and distances are expressed in effective gyroradii). However, we are only interested in the ground mode, which is the most probable to appear because it is the easiest to excite.

Since the collisionless Landau damping of ~1 Hz kinetic Alfvén waves in active regions is much weaker than the collisional one (Voitenko & Goossens 2000), we investigated several collisional dissipation mechanisms for the small-scale torsional Alfvén waves. We found that the waves are damped mainly by Joule heating via resistive dissipation of the field-aligned wave current. The ion viscous dissipation is almost an order of magnitude smaller. The localised heat input, given by the heating function in r, is shown in Fig. 4.

The torsional Alfvén waves propagating in small-scale structures are relevant for the coronal heating problem and can explain the existence and maintenance of interior structures of the loops, locally in places where the density was initially increased. The waves propagate in density threads, damp and heat the plasma. The heat propagates downwards to the photosphere, causing plasma evaporation and sustaining the enhanced density in threads. The positive feedback loop response to the

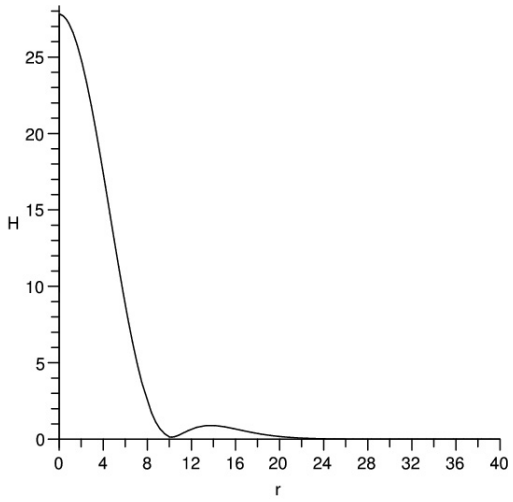

Fig. 4. Heating function in r, made dimensionless by $10^{-9}\sqrt{(\rho_{\rm i}^2+\rho_{\rm s}^2)}/v_{\rm A}\cdot j_z^2$ at $r=0$.

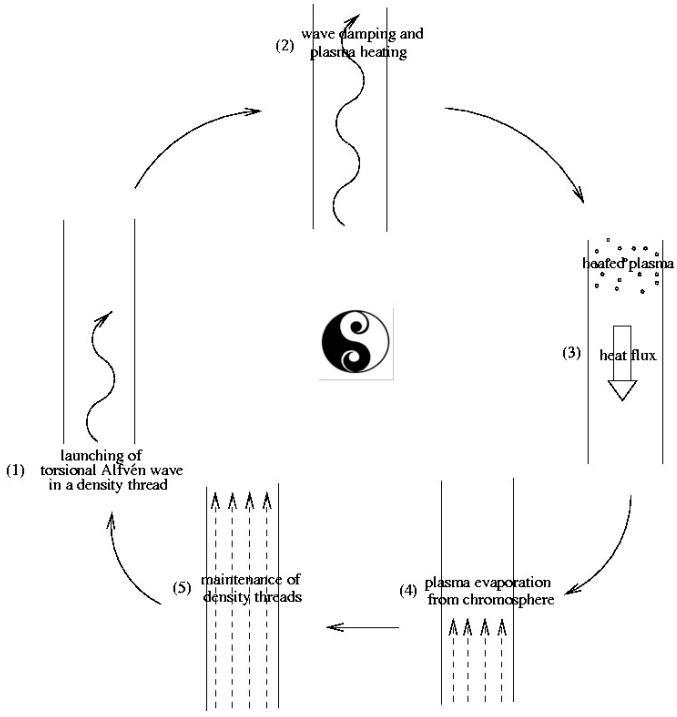

Fig. 5. Sketch of the physical mechanism responsible for the maintenance of density threads.

process (maintenance of density threads) is indicated in Fig. 5. Through this process the structuring of the loop can maintain itself in time, drawing the energy from the photospheric and/or chromospheric sources. What are the factors limiting the density increase, besides the limiting power of the driver excitation Alfvén waves? With increasing density, several processes switch on, which decrease and spread out the localised density enhancements. The most important are plasma diffusion across the magnetic field, away from the threads, and enhanced plasma emission. These processes eventually lead to saturation of the density increase.

In a recent paper, Aschwanden et al. (2007) suggest (and give ten reasons for their statement) that the heating mainly occurs in the transition region/upper chromosphere, from where the plasma evaporates in the corona. The heating mechanism we proposed (by torsional Alfvén waves) does not contradict this suggestion because the wave damping is increased in the places where plasma is more collisional, in the transition region/upper chromosphere. However, more precise calculations should be done taking into account the plasma inhomogeneity along the background magnetic field. If the plasma inhomogeneity along the thread is taken into account, the wave damping and plasma heating should be localised at the footpoints, where the resistivity is larger. In this case, the stages (2) and (3) of Fig. 5 have to be supplemented/replaced with the stage of enhanced heating at the footpoints, in agreement with Aschwanden et al. (2007).

Alternative kinetic excitation mechanisms, similar to that studied by Voitenko & Goossens (2003), can also be efficient for kinetic Alfvén eigenmodes in coronal structures and could provide wave sources in the coronal loops. This problem is under consideration.

Appendix

To obtain Eq. (13) we proceed in the following way: the first step is to eliminate the velocities and densities and obtain two equations in vector potential, A_z, and scalar potential, ϕ; the second step is to eliminate ϕ in order to obtain an equation only in A_z.

The first equation in A_z and ϕ is obtained by expressing $\boldsymbol{v}_{\rm i}$ and $\boldsymbol{v}_{\rm e}$ from the motion equations and replacing them in the condition for solenoidal currents. We describe the details below.

From the perpendicular component of the ion motion Eq. (1), after writing $\boldsymbol{E}$ as a function of scalar and vector potentials (9), and using $p_{\rm i}=nT_{\rm i}$, we can express $v_r^{\rm i}$ as:

$$\left(\frac{\partial^2}{\partial t^2}+\omega_{\rm ci}^2\right)v_r^{\rm i}=-\frac{T_{\rm i}}{n_0M}\frac{\partial^2 n}{\partial t\partial r}-\frac{\rm e}{M}\frac{\partial^2\phi}{\partial t\partial r}. \tag{21}$$

Because $v_r^{\rm e}\ll v_r^{\rm i}$, we take $v_r^{\rm e}=0$. In the parallel direction the ions do not move, so $v_z^{\rm i}=0$, but the much lighter electrons move and their velocity can be calculated from the parallel component of Ampère's law (7):

$$v_z^e=\frac{c}{4\pi n_0{\rm e}}\triangle_\perp A_z. \tag{22}$$

The plasma is electrically neutral, i.e. $n_{\rm i}=n_{\rm e}$, and we denote the perturbed number density for both species by n. We express n from the continuity equation for the electrons as:

$$\frac{\partial n}{\partial t}=-n_0\frac{\partial v_z^{\rm e}}{\partial z}. \tag{23}$$

By replacing (21) and (22) in the equation $\nabla\cdot\boldsymbol{j}=0$ and using also Eq. (23), we obtain:

$$\frac{\partial}{\partial r}\left[r\frac{T_{\rm i}}{M}\frac{\partial^2}{\partial z\partial r}\Delta_\perp A_z-r\frac{4\pi n_0e^2}{cM}\frac{\partial^2\phi}{\partial t\partial r}-\left(\frac{\partial^2}{\partial t^2}+\omega_{\rm ci}^2\right)r\frac{\partial A_z}{\partial r}\right]=0. \tag{24}$$

The second equation in ϕ and A_z is derived by writing the parallel component of the electron continuity equation, in which we neglect the inertial term, but keep the pressure term:

$$0=-T_{\rm e}\frac{\partial n}{\partial z}+n_0{\rm e}\left(\frac{\partial\phi}{\partial z}+\frac{1}{c}\frac{\partial A_z}{\partial t}\right). \tag{25}$$

Using also Eqs. (22) and (23), we get:

$$\left(\frac{\partial^2}{\partial t^2}+\frac{c^2T_{\rm e}}{4\pi n_0e^2}\frac{\partial^2}{\partial z^2}\triangle_\perp\right)A_z+c\frac{\partial^2\phi}{\partial t\partial z}=0. \tag{26}$$

Combining Eqs. (24) and (26) and neglecting the cyclotron effects, we obtain Eq. (13).

References

Aschwanden M. J., & Nightingale, R. W. 2005, ApJ, 633, 499
Aschwanden, M. J., Winebarger, A., Tsiklauri, D., & Peter, H. 2007, ApJ, 659, 1673
Banerjee, D., Teriaca, L., Doyle, J. G., & Wilhelm, K. 1998, A&A, 339, 208
Belcher, J. W., & Davis, L., Jr. 1971, J. Geophys. Res., 76, 3534
Doyle, J. G., Teriaca, J. G., & Banerjee, D. 1999, A&A, 349, 956
Gabriel, A. H. 1974, IAUS, 56, 295
Gordon, B. E., & Hollweg, J. V. 1983, ApJ, 266, 373
Grossmann, W., & Smith, R. A. 1988, ApJ, 332, 476
Harrison, R. A., Hood, A. W., & Pike, C. D. 2002, A&A, 392, 319
Hollweg, J. V. 1990, AGU Geophysical Monograph, 58, 23
Hollweg, J. V., & Yang, G. 1988, J. Geophys. Res., 93, 5424
Kopp, R. A. 1972, Sol. Phys., 27, 373
Kopp, R. A., & Kuperus, M. 1968, Sol. Phys., 4, 212
Ofman, L., & Davila, J. M. 1995, ApJ, 456, L123
Poedts, S., Goossens, M., & Kerner, W. 1989, Sol. Phys., 123, 83
Poedts, S., Goossens, M., & Kerner, W. 1990, ApJ, 360, 279
Reale, F., & Perez, G. 2000, ApJ, 528, L45
Roberts, B., Edwin, P. M., & Benz, A. O. 1984, ApJ, 279, 857
Ruderman, M. S., Berghmans, D., Goossens, M. & Poedts, S., 1997a, A&A, 320, 305
Ruderman, M. S., Goossens, M., Ballester, J. L., & Oliver, R., 1997b, A&A, 328, 361
Spruit, H. C. 1982, Sol. Phys., 75, 3
Vaiana, G. S., Davis, J. M., Giacconi, R., et al. 1973, ApJ, 185, L47
Voitenko Y., & Goossens M. 2000, A&A, 357, 1086
Voitenko Y., & Goossens M. 2003, Space Sci. Rev., 107, 387
Wilhelm, K., Dwivedi, B. N., & Teriaca, L. 2004, A&A, 415, 1133
Zaqarashvili, T. V. 2003, A&A, 309, L15
Zaqarashvili, T. V., & Murawski, K. 2007, A&A, 470, 353